

Hydraulic design of pine needles: one-dimensional optimization for single-vein leaves

MACIEJ A. ZWIENIECKI¹, HOWARD A. STONE², ANDREA LEIGH³, C. KEVIN BOYCE⁴ & N. MICHELE HOLBROOK⁵

¹Arnold Arboretum, Harvard University, 16 Divinity Ave., Cambridge, MA 02138, USA, ²Division of Engineering and Applied Sciences, Harvard University, 29 Oxford St. Cambridge, MA 02138, USA, ³School of Botany and Zoology, The Australian National University, Canberra ACT 0200, Australia, ⁴Department of Geophysical Sciences, University of Chicago, 5734 S. Ellis Ave., Chicago IL 60637, USA and ⁵Organismic and Evolutionary Biology, Harvard University, 16 Divinity Ave., Cambridge, MA 02138, USA

ABSTRACT

Single-vein leaves have the simplest hydraulic design possible, yet even this linear water delivery system can be modulated to improve physiological performance. We determined the optimal distribution of transport capacity that minimizes pressure drop per given investment in xylem permeability along the needle for a given length without a change in total water delivery, or maximizes needle length for a given pressure difference between petiole and needle tip. This theory was tested by comparative analysis of the hydraulic design of three pine species that differ in the length of their needles [*Pinus palustris* (Engl.) Miller, ~50 cm; *Pinus ponderosa* Lawson & Lawson, ~20 cm and *Pinus rigida* Miller, ~5 cm]. In all three species, the distribution of hydraulic permeability was similar to that predicted by the optimum solution. The needles of *P. palustris* showed an almost perfect match between predicted and actual hydraulic optimum solution, providing evidence that vein design is a significant factor in the hydraulic design of pine leaves.

Key-words: model; tracheids; xylem.

INTRODUCTION

How long can a pine needle be? A simple answer to this question is that a needle can only be as long as its vascular system is capable of supplying sufficient water to permit effective photosynthetic function throughout the leaf. While many leaves have complex water distribution systems, pine needles have a very simple design that consists of a single linear vein extending from the base to the tip. Within this vein, the xylem consists entirely of short (100–300 μm long) tracheids (Esau 1977). Water moves axially along the vein and leaks laterally from the xylem through the transfusion tissue and then across the endodermis to the mesophyll where it evaporates into internal air spaces and diffuses out of the leaf through the stomata (Boyer

1985; Kramer & Boyer 1995). The goal of this study was to understand the hydraulic design of this essentially one-dimensional water distribution system.

On first examination, the needle hydraulic design might be thought to be similar to the porous pipe model described for roots (Landsberg & Fowkes 1978; Zwieniecki, Thompson & Holbrook 2002). However, a major difference exists between the two systems. In the case of the root, the entire process is convective and thus the distribution of water uptake along the root depends entirely on the water potential gradients between the xylem and the soil. Because xylem water potentials are ‘applied’ to the root at its proximal (shoot-ward) end, water uptake will be non-uniform along the length of the root (Frensch & Steudle 1989; Zwieniecki *et al.* 2002). If the water-permeable portion of the root (distal unsuberized zone) exceeds in length what is needed to supply the shoot, the root tip may become isolated hydraulically from the transpiration stream. Excessive root length is inefficient in terms of investments in organs for water acquisition, but the root tip is in little danger of desiccation as it can absorb water directly from the soil.

In the case of the needle, water loss is diffusional, driven by the concentration gradient in water vapour between the intercellular air spaces of the leaf and the atmosphere. Because leaf water potential has only a minor effect on the equilibrium vapour pressure (Nobel 1983), the rates of evaporation along the needle will be essentially independent of the pressure within the xylem and instead depend on the driving gradient for vapour diffusion and the conductance of the needle surface to water vapour. Nevertheless, the liquid phase pathway for water movement through leaves does influence the ability of a leaf to support high rates of evaporation through the impact of leaf water status on stomatal aperture. Thus, for a given investment in xylem permeability there is a limit on needle length before the pressure in the xylem reaches the threshold for stomatal closure at the tip. A similar role for the venation in limiting leaf size was proposed as the basis for differences in leaf size and shape within the crown of *Quercus rubra* trees (Zwieniecki, Boyce & Holbrook 2004a). However, leaf vasculature also contributes to the mechanical properties of

Correspondence: Maciej A. Zwieniecki. Fax: +00 617 496 5854; e-mail: mzwienie@oeb.harvard.edu

leaves, and functions in the export of photosynthate. Thus, it is possible that axial permeability exceeds what is needed to efficiently deliver water to evaporation sites (Martre, Cochard & Durand 2001) and that needle size is not limited by its water distribution system.

To explore if the hydraulic system of pine needles evolved to optimize delivery of water per fixed investment in axial permeability, we asked how the hydraulic design of pine needles compares with the distribution of hydraulic permeability needed to maximize needle length or minimize the pressure drop along the vein. The presence of such optimization would suggest that xylem hydraulic properties play an important role in leaf performance, and thus, are a potential constraint on leaf size. The simplicity of the geometry of the pine needle allows for detailed analysis using a formal mathematical approach. Here, we construct a model of the hydraulic system of single-vein leaves and present a mathematical procedure that calculates the optimum distribution of axial hydraulic permeability. We compare theoretical findings with measurements conducted on three species with a wide range of needle length, but exhibiting the same general morphology (i.e. all species have needles in fascicles of three such that the cross-sectional shapes of both the needle and the vascular bundle are similar): *Pinus palustris* (Engl.) Miller in its juvenile stage has needles ranging from 45 to 50 cm in length, *Pinus ponderosa* Lawson & Lawson has needles ranging from 20 to 25 cm in length and *Pinus rigida* Miller produces needles 10–11 cm in length. Our results suggest that xylem hydraulics plays an important role in constraining needle length, especially in species with long needles, and that species optimize their xylem permeability to efficiently use the materials required for constructing xylem conduits.

Theoretical analysis: a model for pressure distribution in the needle

Using cylindrical coordinates, let $z=0$ denote the base of the needle, and $z=l$ denote the tip, where we assume there is no loss of water. Let A be the cross-sectional area of the tracheid lumens, which we assume to be constant in this initial development (Fig. 1 & Table 1). Then we can

Table 1. Units and descriptions of symbols used in the text

Symbol	Units	Descriptions
$A(z)$	(m ²)	Tracheid lumen cross-sectional area
$N(z)$		Number of tracheids
$K(z)$	(m ⁴)	Grand permeability of xylem
Q	(m ³ s ⁻¹)	Total evaporation from the needle
$k(z)$	(m ²)	Darcy's permeability
l	(m)	Needle length
$p(z)$	(Pa)	Hydrostatic pressure
q	(m ³ m ⁻¹ s ⁻¹)	Evaporation rate per needle length
$u(z)$	(m s ⁻¹)	Fluid velocity
	(Pa·s)	Fluid viscosity
z	(m)	Distance from the needle base

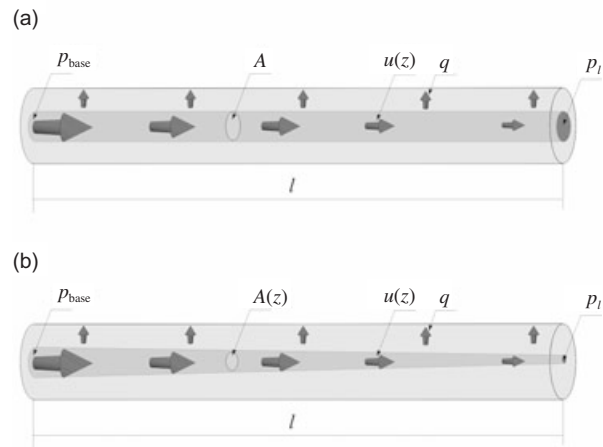


Figure 1. Model representation of a pine needle as a one-dimensional distribution system. (a) Control model of the needle with xylem cross-sectional area independent of length. (b) Model of the needle with xylem cross-sectional area functionally related to distance from the needle base. p_{base} , pressure at the needle base; A , cross-sectional area of the tracheid lumens; $u(z)$, fluid velocity; q , evaporation rate per needle length; p_t , pressure at the needle tip; l , needle length; $A(z)$, tracheid lumen cross-sectional area.

examine a section between z and $z + \Delta z$ and write the mass balance as

$$A[u(z) - u(z + \Delta z)] - q\Delta z = 0, \quad (1)$$

where u denotes the average water velocity, and $q\Delta z$ denotes the evaporation rate out of the leaf section of length Δz . After dividing the mass balance formula by Δz and taking the limit of $\Delta z \rightarrow 0$, we arrive at

$$\frac{du}{dz} = -\frac{q}{A}, \quad (2)$$

Next, we can use Darcy's law for the relationship between u and pressure p in the following form:

$$\frac{dp}{dz} = -\frac{\mu u}{k}, \quad (3)$$

where k is the xylem permeability and μ is the viscosity of the liquid. Now, combining Eqns 2 and 3, and assuming that q , A , and k are constant, we have

$$\frac{d^2 p}{dz^2} = \frac{\mu q}{kA}. \quad (4)$$

This equation can be integrated twice to give

$$p(z) = \frac{\mu q}{2kA} z^2 + c_1 z + c_2. \quad (5)$$

We next apply boundary conditions. At $z=0$, we prescribe the pressure at the needle base $p = p_{base}$. At $z=l$, we assume that there is no fluid flux in the axial direction, so $u = dp/dz = 0$ (i.e. all water flowing into the leaf has evaporated by the distance l). We can now solve Eqn 5 for the two constants c_1 and c_2 , and so we arrive at

$$p(z) = p_{\text{base}} + \frac{\mu q l^2}{2kA} \left[\left(\frac{z}{l} \right)^2 - 2 \frac{z}{l} \right]. \quad (6)$$

The pressure distribution in the vein is parabolic and exhibits a monotonic decay starting with negative pressure (i.e. $p_{\text{base}} < 0$, at $z = 0$ (at the needle base) and decays to $p = p_{\text{base}} - q l^2 / 2kA$ at $z = l$ (the needle tip) where it has zero slope.

Any change in needle length (l) will alter the final pressure distribution in the needle near the tip but not the general shape of the curve. This simple model shows that the pressure distribution in the needle is a result of flow due to the evaporation (q) along the needle.

Because the cross-sectional area of the xylem tissue within the vein was assumed in this first model as constant, we can immediately see that near the tip very low axial flow results in a low pressure drop, while near the base of the needle the much higher water flow is associated with a more pronounced loss in pressure. Thus, we can pose an optimization problem to find the distribution of permeability along the leaf that minimizes the pressure drop for a given investment in conductive tissue.

We can use the aforementioned model, but generalize it to allow for axial variation in permeability and cross-sectional area of the xylem. Let us keep the above notation, but now allow $A(z)$ (the cross-sectional area) and $k(z)$ (the permeability) to vary with distance from the base of the needle. We also assume that q (evaporation rate per needle length) is constant along the length of the needle. For the one-dimensional mass balance, we now have

$$\frac{d}{dz} [A(z)u(z)] = -q. \quad (7)$$

Because q is constant, we can integrate this equation to find

$$A(z)u(z) = -qz + c_3. \quad (8)$$

If we impose the boundary condition of no-fluid flux out of the tip of the needle, $u = 0$ at $z = l$, then we find

$$A(z)u(z) = q(l - z). \quad (9)$$

We use Darcy's law, Eqn 3, and so using the form of velocity distribution just obtained, we have

$$\frac{dp}{dz} = -\frac{\mu q(l - z)}{k(z)A(z)}, \quad (10)$$

which can be integrated to yield the pressure drop along the needle $\Delta p = p_{\text{base}} - p_{\text{tip}}$,

$$\Delta p = \mu q \int_0^l \frac{(l - z)}{k(z)A(z)} dz. \quad (11)$$

Now, let us introduce a 'grand permeability' (K) relating the volume flow rate $Q = A(z)u(z)$ to the pressure gradient, which corresponds to a permeability function $K(z) = k(z)A(z)$, that is,

$$\frac{dp}{dz} = -\frac{\mu Q}{K}. \quad (12)$$

Thus, we have a pressure drop in the form

$$\Delta p = \mu q \int_0^l \frac{(l - z)}{k(z)} dz. \quad (13)$$

If we assume that tracheid dimensions are uniform along the length of the needle [$k(z)$ constant], $K(z)$ will be directly proportional to $A(z)$. Thus, we can introduce a function $N(z)$ for the number of tracheids at position z along the needle, and ask the question: What is the distribution of $N(z)$ that minimizes the pressure drop along the leaf length l subject to the constraint that the total number of tracheids remains constant? In other words, what is the optimal investment in conductivity such that

$$\int_0^l N(z) dz = \text{constant}. \quad (14)$$

It is simplest to address this optimization question by rewriting Eqns 13 and 14 in terms of the relative distance from the tip $s = z/l$. Therefore, we have an optimization question

$$\text{minimize } \int_0^l \frac{1-s}{N(s)} ds = \frac{c \Delta p}{\mu q l^2} \quad \text{subject to } \int_0^l N(s) ds = \text{constant}. \quad (15)$$

This optimization problem may be considered using the calculus of variations. The Euler–Lagrange equation corresponding to the solution of the problem statement in Eqn 15 is

$$\frac{d}{dN} \left(\frac{1-s}{N(s)} \right) = \lambda \quad (16)$$

where λ is a constant to be determined (a Lagrange multiplier). Equation 16 can be integrated and rearranged to obtain

$$N(s) = N(0)(1-s)^{1/2} \quad \text{or} \quad \frac{N(z)}{N(0)} = \left(1 - \frac{z}{l} \right)^{1/2}. \quad (17)$$

Equation 17 represents the optimized grand permeability, equivalent to the distribution of equal-sized tracheids, along the needle. Now, we can contrast the pressure drop in needles with uniform and optimized permeabilities. Firstly, we need to calculate the pressure drop assuming the distribution of tracheids is uniform (i.e. with $N_{\text{uniform}} l = \text{constant}$). From Eqn 15 we have

$$\Delta p_{\text{uniform}} = \frac{\mu q l^2}{c N_{\text{uniform}}} \int_0^1 (1-s) ds = \frac{\mu q l^2}{2c N_{\text{uniform}}}. \quad (18)$$

Similarly, for the optimized distribution we have

$$\Delta p_{\text{min}} = \frac{\mu q l^2}{c N(0)} \int_0^1 (1-s)^{1/2} ds = \frac{2 \mu q l^2}{3c N(0)}. \quad (19)$$

Therefore, taking the ratio of Eqns 18 and 19 and recognizing that the requirement to conserve the total number of tracheids is such that

$$N_{\text{uniform}}l = lN(0) \int_0^1 (1-s)^{1/2} ds \quad \text{or} \quad \frac{N_{\text{uniform}}}{N(0)} = \frac{2}{3}, \quad (20)$$

we find

$$\frac{\Delta p_{\text{min}}}{\Delta p_{\text{uniform}}} = \frac{8}{9}. \quad (21)$$

This result shows that by optimally redistributing tracheids along the length of the needle according to hydraulic principles, there might be a reduction in pressure drop by about 10%.

An alternative optimization question is to find the maximum needle length for a given pressure drop given a fixed vascular investment. We can address this question using Eqn 15 because the maximum leaf length corresponds to the minimum value of $c\Delta p/q^2$. Hence, for fixed Δp , we can determine the value of l corresponding to both N_{uniform} and $N_{\text{optimized}}$. In this case we use Eqn 18 which gives

$$\Delta p = \frac{\mu q l_{\text{uniform}}^2}{2cN_{\text{uniform}}}, \quad (22)$$

while for the optimized distribution (Eqn 19) we have

$$\Delta p = \frac{2\mu q l_{\text{max}}^2}{3cN(0)}. \quad (23)$$

Equations 22 and 23 subject to the requirement that the total number of tracheids is conserved lead to

$$\frac{l_{\text{max}}}{l_{\text{uniform}}} = \left(\frac{9}{8}\right)^{1/3} \quad (24)$$

This result gives an optimized length increase of about 4% resulting from the redistribution of tracheids.

METHODS

Needles of *P. palustris* were collected at Greenwood Plantation, Thomasville, GA, USA, placed in plastic bags with wet tissue inside and sent by overnight delivery to the laboratory where they were used immediately for the determination of flow parameters. *Pinus ponderosa* and *P. rigida* needles were collected at the Arnold Arboretum of Harvard University (Jamaica Plain, Boston, MA, USA), placed in plastic bags with wet tissue inside and transported to the laboratory. The needles were stored in a refrigerator for a maximum of 2 d after collection.

Grand (axial) leaf hydraulic permeability was determined using a simple hydraulic manifold allowing for measurement of flow rate under a known pressure difference. Briefly, the needles were wrapped tightly in parafilm at regular intervals (five each for *P. ponderosa* and *P. rigida*, and nine for *P. palustris*). The needles were then cut underwater close to the proximal end of the parafilm, and forced into a silicon tube connected to a container of water on a balance (sartorius ± 0.01 mg). A leak test was performed by raising the needles above the level of

water on the balance. If there was no gas entry into the tube, the needles were placed underwater in a plastic tub with a water level of 90 cm below the water level on the balance. The portion of the needles connected to the hydraulic system was then cut to exactly 1 cm, and water flow through the 1-cm-long piece was determined. This was then repeated on another section of the needles to determine the distribution of axial permeability as a function of distance from the base. All measurements were done on non-sheathed (i.e. mature, photosynthetic) regions.

Sections (1 cm long) were collected from the same locations along the needles as the hydraulic permeability was determined. From each section, several 20- μ m-thick cross-sections were made, stained in toluidine blue and mounted in glycerol. The prepared slides were photographed immediately at $\times 40$ and $\times 400$ magnification under a light microscope, and the digitized pictures were analysed using ImageJ software. Analysis at $\times 40$ included determination of the circumference of the needles and the area of conductive tissue within the vein. The number of conduits (tracheids) was determined at $\times 400$ on a subsample of the vein (approximately 30% of the total area of the xylem) and recalculated for the whole area of the xylem using 'particle' analysis of ImageJ software. A typical set of pictures used in the analysis of needle dimensions is presented in Fig. 2.

The number of stomata per unit needle length was determined for the two inner (flat) surfaces of 10 needles per species by counting the total number of stomatal rows and the average number of stomata per row based on a sample of three rows in 1-mm-long segments sampled at regular intervals. Analysis of variance (ANOVA) was used to test for differences in stomatal number per length in relation to position along the needles.

RESULTS

The grand permeability of pine needles is not constant, but decreases from the base to the tip in all three species. Using a general formula for the distribution of grand permeability (Eqn 17) with the exponent being the dependent parameter, we fitted the measured data to determine the degree of hydraulic optimization in all three species. In *P. palustris* (long-leaf pine), the exponent for the best fit was 0.49 ($R^2 = 0.979$; SE of estimate = 0.0467; 95% confidence interval 0.38–0.61), which is not significantly different from $1/2$, as predicted by the optimal distribution of permeability. The fitted exponent for *P. ponderosa* was 0.58 ($R^2 = 0.986$; SE of estimate = 0.0425; 95% confidence interval 0.47–0.69), a value slightly off the optimum distribution of hydraulic permeability, but within the confidence interval. For *P. rigida*, the exponent was 0.78 ($R^2 = 0.949$; SE of estimate = 0.082; 95% confidence interval 0.55–1.01), a value significantly different from the optimum value (Fig. 3).

A similar analysis, but this time using the number of tracheids instead of axial permeability, was also performed. As expected, the number of tracheids decreased

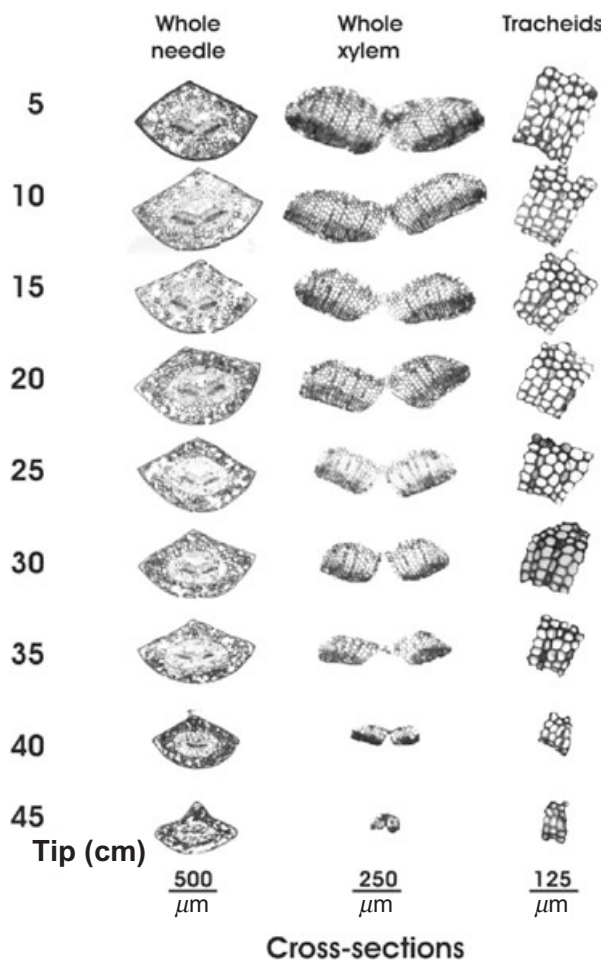


Figure 2. Series of cross-sections of *Pinus palustris* used in the analysis of tracheid number as a function of length, needle cross-sectional area and xylem cross-sectional area. A similar series was collected for the two other species.

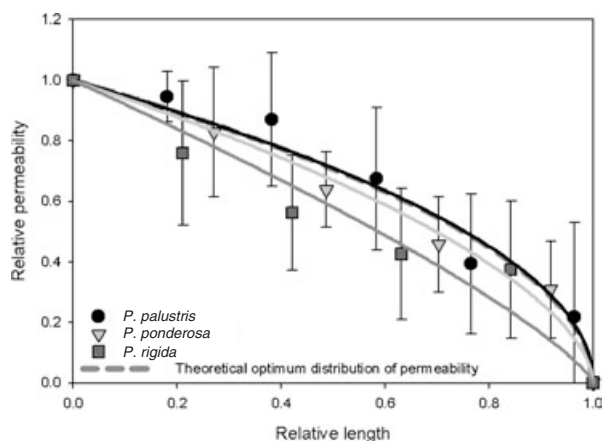


Figure 3. Measured axial distribution of grand hydraulic permeability of needles with fitted function based on Eqn 17 (see text). Optimum theoretical distribution is plotted as a reference line. The values were normalized to those of the leaf base ($z = 0$), where the absolute values for *Pinus palustris*, *Pinus ponderosa* and *Pinus rigida* were $3.37e^{-17}$, $1.77e^{-17}$ and $1.10e^{-17}$ m⁴, respectively. Error bars represent SD.

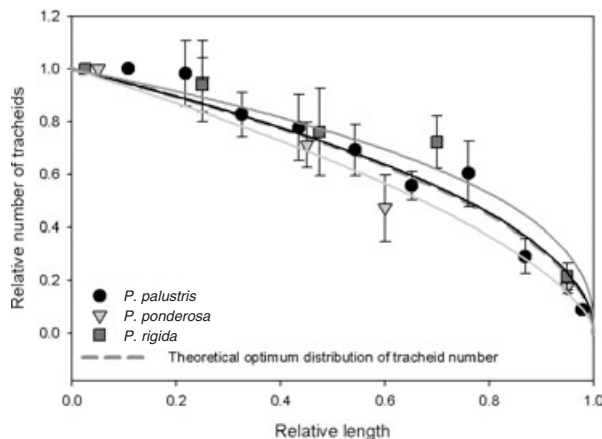


Figure 4. Measured axial distribution of tracheid number with fitted function based on Eqn 17. Optimum theoretical distribution is plotted as a reference line. The values were normalized to those of the leaf base ($z = 0$), where the absolute values for *Pinus palustris*, *Pinus ponderosa* and *Pinus rigida* were 290, 337 and 211, respectively. Error bars represent SD.

from the base towards the tip of the needle. In *P. palustris*, the exponent for the best fit was 0.49 ($R^2 = 0.975$; SE of estimate = 0.0668; 95% confidence interval 0.33–0.65), which is not significantly different from $1/2$ as predicted by the optimal distribution of permeability. The *P. ponderosa* exponent was 0.62 ($R^2 = 0.949$; SE of estimate = 0.0778; 95% confidence interval 0.37–0.87), a value slightly off the optimum distribution of hydraulic permeability, but within the confidence interval. For *P. rigida*, the exponent was 0.40 ($R^2 = 0.945$; SE of estimate = 0.0725; 95% confidence interval 0.17–0.63), also within the confidence interval for the optimum ($1/2$) value (Fig. 4). The analysis of the optimal distribution of tracheid number assumes that tracheid dimensions remain constant. In all three species, the ratio of xylem area to number of tracheids, a proxy for average tracheid dimension, does not differ by more than 10% over 80% of the needle length (Fig. 5). Only at the tip of the needle is there a significant decrease in the xylem area: tracheid number ratio.

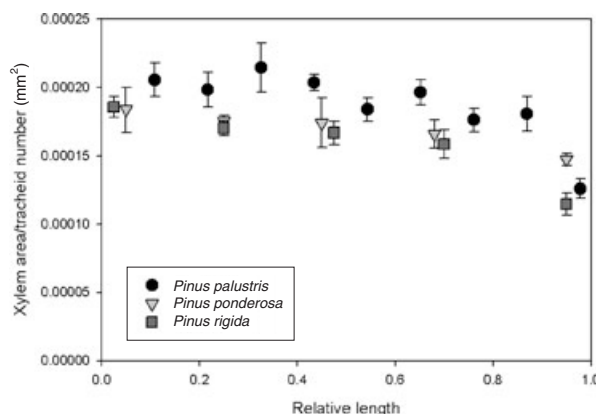


Figure 5. Ratio of xylem area to number of tracheids as a function of position along the needle. Error bars represent SD.

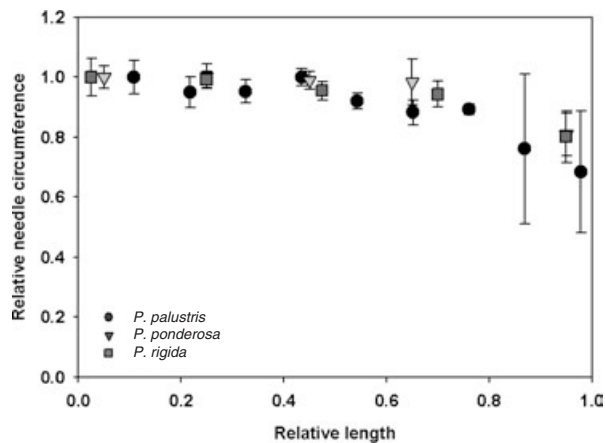


Figure 6. Measured axial circumference of needles as a function of length. The values were normalized to those of the leaf base ($z = 0$), where the absolute values for *Pinus palustris*, *Pinus ponderosa* and *Pinus rigida* were 3.52, 4.08 and 3.20 mm, respectively. Error bars represent SD.

One of the assumptions of our model is that evaporation rate per unit length is constant along the length of the needle. Because evaporation is proportional to surface area and stomatal conductance, a constant needle circumference and a constant stomatal density would be consistent with water loss rates being uniform along the needle. Our results show that needle taper was minimal and only apparent at the very tip of the needle. For almost 80% of the needle length, the taper was <5% with an abrupt change at 95% of the needle length where the circumference dropped to approximately 80% of its initial value (Fig. 6). There were no significant differences in stomatal number per length (per millimetre) as a function of position along the needle in all three species: *P. palustris* (ANOVA: mean = 59.83, $F_{1,61} = 1.258$, $P = 0.266$); *P. ponderosa* (ANOVA: mean = 38.92, $F_{1,38} = 0.011$, $P = 0.916$) and *P. rigida* (ANOVA: mean = 56.38, $F_{1,37} = 0.696$, $P = 0.409$). In addition, the distance between the vascular bundle and the leaf surface remains relatively constant along the needle, suggesting that the radial hydraulic pathway linking xylem with stomata does not vary with position.

DISCUSSION

Single-vein leaves represent the simplest possible hydraulic design in nature apart from leafy structures that entirely lack veins. Despite its apparent simplicity, the vein is not simply a pipe that delivers water from point 'a' to point 'b', but is rather a porous pipe that distributes water along its length. The fact that the vein functions as a porous pipe has important implications for the analysis of the hydraulic design of needles. One of the inevitable properties is that the pressure drop in the vein is a combination of vein permeability and water loss due to leakage out of the vein (Eqn 5) and thus not simply the effect of water viscosity and radius as predicted by Poiseuille's law. Increasing axial permeability decreases the pressure drop per length while

increasing the leak (evaporation) increases the pressure gradient. Thus, to predict correctly the distribution of pressure within the vein, we need to know water loss due to evaporation and axial vein permeability. However, because evaporation is governed by the diffusive resistance imposed by the stomata, we do not need to know the radial resistance for water flow out of the vein in order to calculate the pressure distribution within the xylem (Eqn 6) – a situation that contrasts with the analysis of water flow in roots (Landsberg & Fowkes 1978; Frensch & Steudle 1989; Zwieniecki *et al.* 2002).

In an earlier study, we examined the impact of radial and mesophyll resistances (in addition to axial and stomatal resistances) on the shape of single-vein leaves (Zwieniecki, Boyce & Holbrook 2004b). In that study, evaporation rates were assumed to be constant across the leaf surface, with a fixed pressure drop dictating stomatal closure being used to determine the leaf shape that could be supplied by this combination of hydraulic parameters. Within each simulation, the hydraulic parameters were fixed (i.e. not allowed to vary as a function of position within the leaf). Not surprisingly, radial and mesophyll resistances had a large effect on leaf shape.

By contrast, in this study we focus exclusively on how investments in axial permeability should be arrayed along the length of the needle to maximize needle length with a fixed needle-like shape. We used equal-sized tracheids as a proxy for investment in axial permeability, allowing us to extend the analysis of grand permeability to needle structure. The assumption of equal-sized tracheids holds for much of the needle, but diverged to some degree at the very tip. We recognize that the hydraulic properties governing water movement radially out of the vascular bundle and across the mesophyll may influence rates of evaporation from the leaf surface via their effect on epidermal water status and stomatal aperture. However, this will not influence the analysis presented here as long as our assumption of uniform evaporation rates along the length of the needle holds. Thus, recent discussions as to the relative magnitude of the hydraulic resistance imposed by water flow through venation versus across the mesophyll (e.g. Cochard, Nardini & Coll 2004; Sack, Streeter & Holbrook 2004; Sack & Holbrook 2005) are not relevant to the question of how investments in axial permeability should be optimally distributed. The assumption that evaporation rates are constant along needle length reflects the idea that leaves should be supplied with water in such a way as to allow their entire surface area to function equally well in CO_2 uptake (Roth-Nebelsick *et al.* 2001; Sack *et al.* 2003). Anatomical and morphological measurements of the three species are consistent with this assumption, demonstrating a little change in the surface area (needle circumference) and in stomatal number per length as a function of distance from the base of the needle.

Our model suggests that a minimum drop in pressure along the leaf axis for a given investment in conductive tissue requires hydraulic permeability to be distributed

along the leaf length as predicted by Eqn 17. This results in an approximately 10% reduction in pressure dissipation along the axis of the needle. Although this reduction seems relatively small, it allows for the production of additional photosynthetic surface (4%) in the most light-exposed location. The estimated parameter describing the distribution of permeability (0.49) was surprisingly close to the predicted value of $1/2$ in the species with the longest needles (*P. palustris*), and it was matched with conduit distribution where the exponent was estimated to be also 0.49. This suggests that the axial hydraulic component of water flow in needles of *P. palustris* might be an important design feature of the leaf, consistent with the idea that the vein is not hydraulically overbuilt.

In the two species with shorter needles, the tracheid distribution was close to that predicted by the model, although the distribution of axial permeability in *P. rigida* did not match the optimum distribution predicted by the model. This potentially indicates a diminishing role for xylem hydraulics in shorter needles, allowing for other traits to dominate leaf design. This result might come as no surprise because *P. rigida* grows naturally in environments where wind and snow are important mechanical stresses that might cause hydraulic design to be less important for survival. Despite this aspect, the tracheid distribution followed the model predictions, suggesting that even in short needles there is some optimization of the hydraulic system.

It is interesting to consider the optimum distribution of tracheids and permeability in pine needles in the context of leaf development. Pine needles grow using an intercalary meristem located at the base of the needle. The activity of this meristem propels the tip away from the growth zone, where it becomes mature and loses its ability to change its structure. Newly formed tissues at the base of the needle are constructed in such a way that the hydraulic permeability is increased in parallel with the optimum distribution predicted by our model. This poses an intriguing question of information exchange between the already mature portion of the needle and the growth zone. The hydraulic design of pine needles, thus, appears highly predetermined, with the final structure depending on both transpiration rates and initial permeability close to the tip. Nevertheless, the final length of the needle is likely to reflect environmental conditions that influence water loss rates, as was found for oak leaves (Zwieniecki *et al.* 2004b).

ACKNOWLEDGMENTS

This research was supported by The Andrew W. Mellon Foundation, Harvard MRSEC (DMR-0213805) and the

National Science Foundation (Grant # 0106816, 0517071). We are grateful to Sean Coyne of Greenwood Plantation for providing the long-leaf pine material. We also would like to thank Joshua Weitz for discussion and useful comments.

REFERENCES

- Boyer J.S. (1985) Water transport. *Annual Review of Plant Physiology* **36**, 473–516.
- Cochard H., Nardini A. & Coll L. (2004) Hydraulic architecture of leaf blades: where is the main resistance? *Plant, Cell and Environment* **27**, 1257–1267.
- Esau K. (1977) *Anatomy of Seed Plants*, 2nd edn. John Wiley & Sons, New York, USA.
- Frensch J. & Steudle E. (1989) Axial and radial hydraulic resistance to roots of maize (*Zea mays* L.). *Plant Physiology* **91**, 719–726.
- Kramer P.J. & Boyer J.S. (1995) *Water Relations of Plants and Soils*. Academic Press, San Diego, CA, USA.
- Landsberg J.J. & Fowkes N.D. (1978) Water movement through plant roots. *Annals of Botany* **42**, 493–508.
- Martre P., Cochard H. & Durand J.-L. (2001) Hydraulic architecture and water flow in growing grass tillers (*Festuca arundinacea* Schreb.). *Plant, Cell and Environment* **24**, 65–76.
- Nobel P.S. (1983) *Biophysical Plant Physiology and Ecology*. W.H. Freeman, New York, USA.
- Roth-Nebelsick A., Uhl D., Mosbrugger V. & Kerp H. (2001) Evolution and function of leaf architecture: a review. *Annals of Botany* **87**, 533–566.
- Sack L. & Holbrook N.M. (2005) Leaf hydraulic architecture correlates with regeneration irradiance in tropical rainforest trees. *New Phytologist* **164**, 403–413.
- Sack L., Cowan P., Jaikumar N. & Holbrook N. (2003) The ‘hydrology’ of leaves: coordination of structure and function in temperate woody species. *Plant, Cell and Environment* **26**, 1343–1356.
- Sack L., Streeter C.M. & Holbrook N.M. (2004) Hydraulic analysis of water flow through leaves of *Acer saccharum* and *Quercus rubra*. *Plant Physiology* **134**, 1824–1833.
- Zwieniecki M.A., Thompson M.V. & Holbrook N.M. (2002) Understanding the hydraulics of porous pipes – tradeoff between water uptake and root length utilization. *Journal of Plant Growth Regulators* **21**, 315–323.
- Zwieniecki M.A., Boyce C.K. & Holbrook N.M. (2004a) Hydraulic limitations imposed by crown placement determine final size and shape of *Quercus rubra* L. leaves. *Plant, Cell and Environment* **27**, 357–365.
- Zwieniecki M.A., Boyce C.K. & Holbrook N.M. (2004b) Functional design space of single-veined leaves: role of tissue hydraulic properties in constraining leaf size and shape. *Annals of Botany* **94**, 507–513.

Received 23 June 2005; received in revised form 21 August 2005; accepted for publication 25 August 2005